fermentation

MDPI

Article

Palm Oil Mill Effluent for Lipid Production by the Diatom *Thalassiosira pseudonana*

Karthick Murugan Palanisamy [1], Gaanty Pragas Maniam [1,2], Ahmad Ziad Sulaiman [3], Mohd Hasbi Ab. Rahim [1], Natanamurugaraj Govindan [1] and Yusuf Chisti [4,*]

[1] Algae Biotechnology Laboratory, Faculty of Industrial Sciences and Technology, Universiti Malaysia Pahang, Lebuhraya Tun Razak, Gambang, Kuantan 26300, Pahang, Malaysia; karthickmurugan13395@gmail.com (K.M.P.); gaanty@ump.edu.my (G.P.M.); mohdhasbi@ump.edu.my (M.H.A.R.); natanam@ump.edu.my (N.G.)

[2] Centre for Research in Advanced Tropical Bioscience, Universiti Malaysia Pahang, Lebuhraya Tun Razak, Gambang, Kuantan 26300, Pahang, Malaysia

[3] Faculty of Bioengineering and Technology, Universiti Malaysia Kelantan, Jeli 17600, Kelantan, Malaysia; ziad@umk.edu.my

[4] School of Engineering, Massey University, Private Bag 11 222, Palmerston North 4442, New Zealand

* Correspondence: Y.Chisti@massey.ac.nz

Abstract: Biomass and lipid production by the marine centric diatom *Thalassiosira pseudonana* were characterized in media based on palm oil mill effluent (POME) as a source of key nutrients. The optimal medium comprised 20% by volume POME, 80 μM Na_2SiO_3, and 35 g NaCl L^{-1} in water at pH ~7.7. In 15-day batch cultures (16:8 h/h light–dark cycle; 200 μmol photons m^{-2} s^{-1}, 26 ± 1 °C) bubbled continuously with air mixed with CO_2 (2.5% by vol), the peak concentration of dry biomass was 869 ± 14 mg L^{-1} corresponding to a productivity of ~58 mg L^{-1} day^{-1}. The neutral lipid content of the biomass was 46.2 ± 1.1% by dry weight. The main components of the esterified lipids were palmitoleic acid methyl ester (31.6% *w*/*w*) and myristic acid methyl ester (16.8% *w*/*w*). The final biomass concentration and the lipid content were affected by the light–dark cycle. Continuous (24 h light) illumination at the above-specified irradiance reduced biomass productivity to ~54 mg L^{-1} day^{-1} and lipid content to 38.1%.

Keywords: *Thalassiosira pseudonana*; palm oil mill effluent; diatom lipids; algal biodiesel

Citation: Palanisamy, K.M.; Maniam, G.P.; Sulaiman, A.Z.; Ab. Rahim, M.H.; Govindan, N.; Chisti, Y. Palm Oil Mill Effluent for Lipid Production by the Diatom *Thalassiosira pseudonana*. *Fermentation* **2022**, *8*, 23. https://doi.org/10.3390/fermentation8010023

Academic Editor: Diomi Mamma

Received: 10 December 2021
Accepted: 30 December 2021
Published: 10 January 2022

1. Introduction

Palm oil is globally the most widely consumed vegetable oil. Palm oil is produced in tropical regions such as Indonesia, Malaysia, and Thailand. The processing of palm oil generates nutrient-rich wastewater known as palm oil mill effluent or POME. Each metric ton of palm oil produced generates between 2.5 and 3 tons of POME [1,2]. POME does not contain any nonbiodegradable material, but its untreated discharge is a major source of pollution in some regions [1,2].

Microalgae, including diatoms, are sources and potential sources of diverse products [3–7] including edible oils. POME can be used as a cheap source of some nutrients in culture media for growing microalgae to produce various possible products, including biomass for aquaculture feed, natural colorants such as astaxanthin, and polyunsaturated fatty acids such as docosahexaenoic acid [4,5]. POME also contains metabolizable dissolved organic compounds. Absorption of nutrients from POME by microalgae can reduce its polluting potential [5,8,9]. POME-based culture media have supported good growth of diverse microalgae including diatoms such as *Chaetoceros affinis* [10], *Gyrosigma* sp. [11], *Amphora copulata* [12], and *Amphora* sp. [13]. POME cannot be used undiluted in algal culture media because of two factors: the dark color of undiluted POME prevents the algal cells from accessing light [10] and certain compounds naturally present in POME inhibit the growth of algal cells if added in a high concentration [14–16].

Diatoms are of particular interest as producers of high-value lipids [6,7,11,12,17,18]. Diatoms accumulate neutral lipids such as triacylglycerols typically in oil bodies [19]. *Thalassiosira pseudonana* (Bacillariophyceae) (formerly *Cyclotella nana* [20]) is a widely studied model diatom with a fully sequenced genome [21,22], but it has not been examined for lipid production in POME-based culture media. Therefore, *T. pseudonana* was the focus of the present study. Each cell of *T. pseudonana* typically accumulates 3 to 5 oil bodies that range in size from 0.3 to 1.5 µm [19]. For diatom culture, POME can supply all the required inorganic nitrogen, phosphorous, trace elements, and vitamins [10], but it lacks sufficient silicate, a mineral required by the diatoms to build cell walls [23,24].

Diatoms growing photoautotrophically thrive only on light and inorganic nutrients. In addition, many diatoms are able to utilize dissolved organic compounds for carbon and energy in combination with light (mixotrophy), or in the dark (heterotrophy) [10,25]. Thus, organic carbon present in POME may also be utilized by some diatoms. Specifically, *T. pseudonana* is known to metabolize organic carbon sources including glucose, acetate, and glycerol for growth [26]. Mixotrophic growth simultaneously using carbon dioxide, organic carbon, and light has enhanced biomass productivity compared to exclusively photoautotrophic growth in microalgae capable of internalizing and metabolizing organic carbon sources [27].

The light–dark cycle has been shown to affect the growth, physiology, and molecular dynamics of *T. pseudonana* [28,29] as well as other diatoms [30]. High light stress has been linked to observable proteomic responses [31]. The intensity of incident light affects the proportion of polyunsaturated fatty acids in the total lipids of the diatom [32]. In addition, the relative proportions of the lipid classes and the specific fatty acids in rapidly growing cells can be different compared to cells in a stationary state [33,34].

T. pseudonana is generally considered a marine diatom although its natural distribution spans both marine and freshwater habitats, apparently because of its freshwater ancestry [35]. This diatom is globally widespread [35–41]. The diatom is able to grow at a broad range of temperatures (e.g., 4–28 °C), but the growth rate is maximum around 28 °C [42]. Sparging the culture with a 5% vol/vol level of carbon dioxide in air supports better photoautotrophic growth compared to lower levels of carbon dioxide [43]. Aeration also provides the oxygen required for growth on organic carbon in the dark.

An irradiance level of ~400 µmol photons m^{-2} s^{-1} saturates photosynthesis without causing photoinhibition in *T. pseudonana* [44]. Volumetric biomass productivity of around 80 mg L^{-1} day^{-1} has been reported in a semi-continuous culture of this diatom at 22 °C [44]. In addition to silicon, *T. pseudonana* requires selenium for growth [45]. Selenium deficiency interferes with cell division and results in ultrastructural changes in the membrane systems of mitochondria and chloroplasts [46]. A sodium selenite (Na_2SeO_3) concentration of 10^{-10} M supports good growth, but $\geq 10^{-3}$ M inhibits it [45]. In seawater, Se is naturally present at a concentration of around 5.1×10^{-8} M. *T. pseudonana* is commercially used as an aquaculture feed [47–49] where it is a source of certain dietary fatty acids.

Thalassiosira pseudonana strain used in the present study was isolated from tropical coastal waters of Kuantan, peninsular Malaysia. The diatom was cultured in a medium formulated with POME as a source of all nutrients except silicon. The focus was on identifying the optimal concentration of POME as the main source of nutrients (nitrogen, phosphorous, vitamins, trace elements) in the culture medium without compromising the biomass productivity relative to a standard control medium. In addition, in media with identified optimal concentration of POME, the optimal level of silicon was identified as POME is deficient in silicon. Once the medium had been optimized, the diatom was cultured under various light–dark cycles, to determine the optimal cycle for maximal growth. The most productive culture medium and light–dark cycle were used to characterize biomass growth, lipid production, and the lipid profile.

2. Materials and Methods

2.1. Microscopic Characterization

Thalassiosira pseudonana strain had been isolated from coastal waters of Kuantan region, peninsular Malaysia, as previously reported [10]. Microscopic examination (Olympus BX53 fluorescence microscope; Olympus Corporation, Tokyo, Japan) and field emission scanning electron microscopy (Jeol JSM-7800F FESEM; JEOL USA, Inc., Peabody, MA, USA) of cleaned frustules (silicified cell wall) were used to confirm its identity with reference to published classification keys [50–53]. Isolation, preparation, and analysis followed the standard protocols [54].

Cleaned frustules for morphological characterization were recovered as described by others [55,56]. Briefly, the cells were recovered by centrifugation (1100× *g*, 5 min) from a 15 mL sample of pure culture. The supernatant was discarded and the pellet was washed by resuspending in 15 mL of distilled water and recovered, as above. The pellet was transferred to a clean test tube, 0.1 g of sodium dichromate was added mixed with 40 mL of 10% aqueous hydrochloric acid. This slurry was mixed and incubated at 60 °C for 10 min in a water bath. The slurry was then left overnight at room temperature on a mixing platform. The suspension was then centrifuged (180× *g*, 5 min) and the supernatant was removed by pipetting. A portion of the pellet was transferred to a glass slide and dried at 60 °C for 10 min for microscopic examination. The cleaned frustules were coated with a thin layer of platinum and imaged using the earlier specified field emission scanning electron microscope.

2.2. Maintenance and Inoculum Preparation

Pure cultures of *Thalassiosira pseudonana* were maintained in 1 L Erlenmeyer flasks in f/2 medium [57] supplemented with 10 nM sodium selenite (Na_2SeO_3). Cultures were continuously sparged (0.4 L min^{-1}) with filter-sterilized air mixed with 2.5% by volume CO_2. The cultures were incubated at 26 ± 1 °C under continuous cool white fluorescent light (90 µmol photons m^{-2} s^{-1}). Inocula were grown as specified above for 14 days.

2.3. Characterization of Palm Oil Mill Effluent

Palm oil mill effluent (POME) samples (10 L) were collected from the final discharge stage of anaerobic treatment ponds of an oil palm mill located in Gambang (3.6197° N, 103.1604° E), Malaysia. The samples were filtered through a final sieve (70 mesh, 212 µm nominal) to remove suspended solids. The physicochemical properties of POME were measured according to standard methods [58]. The characteristics of filtered raw POME are shown in Table 1. Before use in culture media, the filtered POME was diluted with an equal volume of distilled water and autoclaved (121 °C, 20 min). The pH was adjusted to 7.4 ± 0.2 using 1 M NaOH. For preparing the POME-based culture media, the required volume of sterile POME was mixed with distilled water, and salts were added to the required concentration (40–160 µM final concentration of Na_2SiO_3; 35 g NaCl L^{-1}).

Table 1. Physicochemical characteristics of POME [a].

Parameter	Value
pH	5.2 ± 0.9
Ammoniacal nitrogen, NH_3-N (mg L^{-1})	16.3 ± 2.1
Biochemical oxygen demand, BOD (mg L^{-1})	2600 ± 325
Chemical oxygen demand, COD (mg L^{-1})	2664 ± 21
Total nitrogen (mg L^{-1})	141.4 ± 15.3
Total phosphorus (mg L^{-1})	21.5 ± 1.4
Total suspended solids (mg L^{-1})	94.6 ± 5.3

[a] Selenium concentration in POME has been reported to be 1.6 × 10^{-7} M [59].

2.4. Culture Conditions

The effects of medium composition (POME levels of 10–30% by volume; sodium silicate (Na_2SiO_3) concentration of 40–160 μM; 35 g NaCl L^{-1} culture medium) on biomass growth was examined in an initial set of experiments. A total of 16 experiments excluding replicates were performed, grouped in 4 sets (A, B, C, and D) based on different levels of POME and sodium silicate in the culture medium (Table 2). The alga was grown in batch culture in each medium for up to 18 days. Continuous illumination was used (24 h; 200 μmol photos m^{-2} s^{-1}; cool fluorescent light; Philips Malaysia, Selangor) in all cases. The culture temperature was 26 ± 1 °C. Cultures were carried out aseptically in Erlenmeyer flasks (total volume = 1 L; initial culture volume = 20 mL). Immediately after inoculation, the concentration of the algal cells in each flask was 5.0×10^5 cells mL^{-1} (optical density (665 nm) ≈ 0.1). Filter sterilized air containing 2.5% by volume carbon dioxide was used to continuously sparge each culture flask at a flow rate of 0.4 L min^{-1}. All experiments were in triplicate.

Table 2. Compositions of the media.

Experiment Set [a]	POME (% *v*/*v*)
A (40 μM Na_2SiO_3)	0 (control) [b]
	10
	20
	30
B (80 μM Na_2SiO_3)	0 (control) [b]
	10
	20
	30
C (120 μM Na_2SiO_3)	0 (control) [b]
	10
	20
	30
D (160 μM Na_2SiO_3)	0 (control)
	10
	20
	30

[a] All media contained 35 g NaCl L^{-1}. [b] The control was f/2 medium (supplemented with 25 μM sodium silicate and 10 nM sodium selenite).

Once a suitable concentration of POME and sodium silicate had been established based on the above experiments, the identified optimal medium composition was used to investigate the effects of the light–dark cycle on biomass growth. The culture temperature, illumination, aeration, and inoculation levels were the same as in all earlier experiments. Only the light–dark cycle varied (24:0, 16:8, 12:12, and 8:16 h:h) in different experiments.

2.5. Growth Measurements

Optical density (OD_{665}) of the diluted culture measured spectrophotometrically at a wavelength of 665 nm was used to characterize biomass growth. The optical density of serial dilutions of a culture with a biomass concentration that had been determined precisely by gravimetry was used to obtain the following calibration equation:

$$\text{Dry biomass concentration} \left(\text{mg L}^{-1} \right) = 687.91 \times \text{OD}_{665} \quad (1)$$

The above equation was used to convert the routine measurements of sample OD_{665} to a dry biomass concentration.

2.6. Lipid Extraction and Transesterification

Lipids were extracted from a known quantity of dry biomass of the diatom using a published method [60,61]. Briefly, dry biomass was suspended in hexane, vortexed for 3 min, and left standing for 3 h at room temperature. The extraction vessel was then held in an ultrasonic bath (700 W sonication power) at a controlled temperature of 60 ± 1 °C for 1 h. The suspension was then cooled to room temperature and the solids were removed by centrifugation (5000× *g*, 10 °C, 15 min). The residual solids were extracted with hexane a second time, as above. The hexane extracts were pooled and the solvent was evaporated in a fume hood to recover the lipids. The recovered lipids were weighed.

The recovered lipids were transesterified using a published method [62] to produce methyl esters. Briefly, 1.5 g lipid was mixed with 1 mL of methanol containing KOH (10 g L^{-1}) in a 2 mL Eppendorf tube and incubated on a 60 °C water bath for 1 h. Afterward, the mixture was vortexed for 2 min and left standing at room temperature for 1 h and the upper layer was recovered [63].

2.7. Lipid Composition Analysis

A measured quantity of the methyl ester sample was dissolved in octane to obtain a concentration of around 15 mg mL^{-1}. This sample was analyzed by gas chromatography-mass spectroscopy (GC-MS, Agilent 7890A; www.agilent.com). A high polarity MEGA-WAX MS capillary column (0.5 µm film thickness, 0.32 mm internal diameter, 30 m long) was used. The injection volume was 1 µL and the split ratio was 50:1. Helium (1.5 mL min^{-1}) was the carrier gas. The column temperature was 230 °C. Chromatographic peaks were identified by comparing retention times with those of standards. Methyl esters were quantified based on the area of their chromatographic peaks [11].

3. Results and Discussion

3.1. Diatom Identification

The isolated diatom (Figure 1) was easily identified as *Thalassiosira pseudonana* based on the morphological features (general morphology, valve (theca) diameter, number of rimoportulae) seen in field emission scanning electron microscopic images of the cleaned frustules. Patterns on valve surfaces and their finer details (e.g., number of nodes in the ridge pattern, branch lengths, mesh area [50]) revealed in highly magnified images (Figure 1) further confirmed the identity of this well-known diatom [21,36,40,64].

The distinguishing features of the species were a roughly cylindrical shape of the cell with a rectangular, or square side view (or girdle view) (Figure 1A); radially symmetric, centric valves (Figure 1B) consistent with earlier observations [39]; a frustule made up of two overlapping cylindrical halves, the thecae, or valves, fitting together like a box and its lid (Figure 1C); the overlapping region of the two valves showing a series of girdle bands, or siliceous strips that ran along the cylindrical perimeter (Figure 1C,D). The cells expanded by synthesizing girdle bands during cell division [65] but were also capable of sexual reproduction [41,66]. The cells had a large central vacuole (Figure 1A), consistent with other reports [40], and the cytoplasm lined the inner surfaces of the frustule. The cells lacked a raphe system and were nonmotile.

3.2. Effect of POME and Silicate Concentration on Biomass Production

Control cultures were grown in f/2 medium supplemented with sodium silicate and sodium selenite under the conditions specified earlier for comparison with POME-based media. POME-based media all contained the specified quantities of POME and sodium silicate, 35 g NaCl L^{-1}, but no selenite, in distilled water. The diatom growth curves in different media are shown in Figure 2.

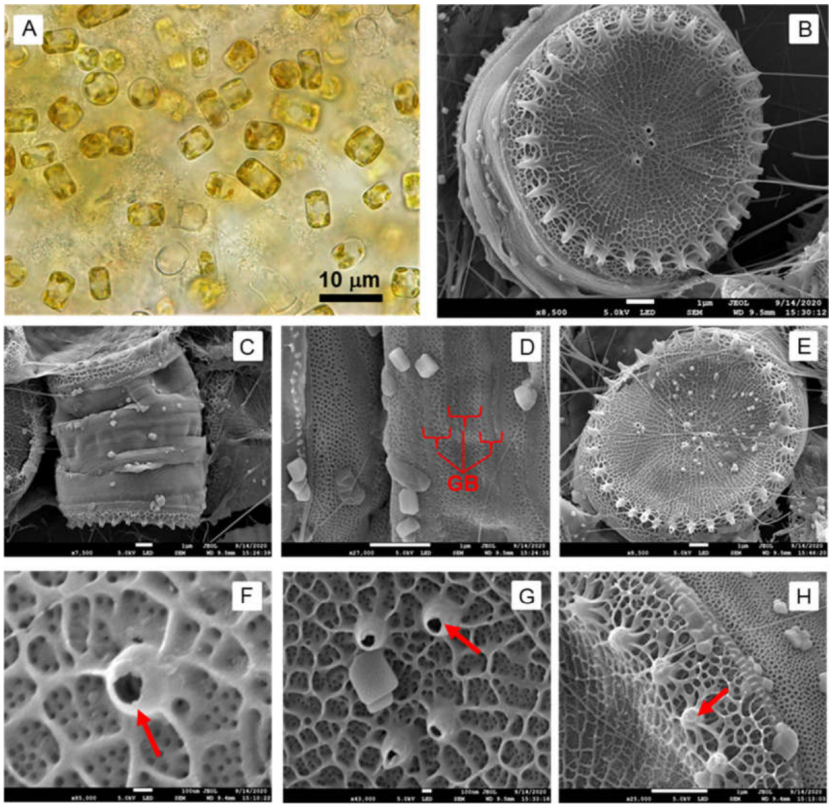

Figure 1. Morphological features of the diatom. Fluorescence microscopic image (100× magnification; bar = 10 µm) (**A**) and FESEM images: 8500× magnified valve view (bar = 1 µm) (**B**); 7500× magnified girdle view (bar = 1 µm) (**C**); 27,000× magnified girdle region (girdle bands are marked as GB) (bar = 1 µm) (**D**); 8500× magnified valve view (bar = 1 µm) (**E**); 85,000× magnified valve central region (bar = 100 nm) (**F**); 43,000× magnified valve central surface (bar = 100 nm) (**G**); 25,000× magnified valve peripheral region (bar = 1 µm) (**H**). Rimoportulae (marked by red arrows) are the protruding tube-like structures located in the central region and the periphery of the valves (**B**,**E**–**H**).

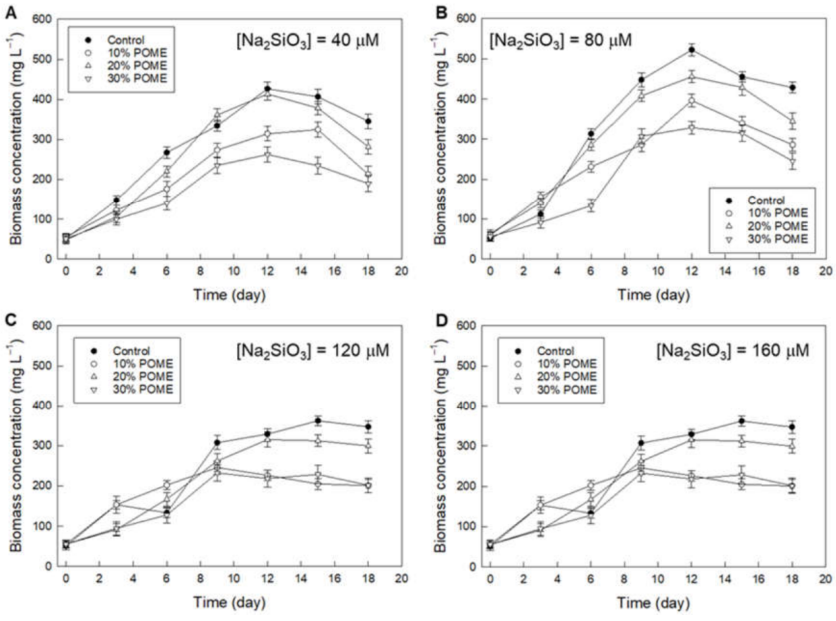

Figure 2. Biomass growth profiles in different media under continuous illumination (200 µmol photons m^{-2} s^{-1}). Initial concentrations of sodium silicate (Na_2SiO_3) were (**A**) 40 µM; (**B**) 80 µM; (**C**) 120 µM; (**D**) 160 µM. Data are mean values ± standard deviation (n = 3).

A medium with 20% POME by volume, 80 μM of Na_2SiO_3, and 35 g NaCl L^{-1} in distilled water proved to be as good as the control medium in providing a high final biomass concentration of 455 ± 10 mg L^{-1} on day 15 (Figure 2B). Compared to a POME level of 20%, both higher and lower POME concentrations reduced biomass production (Figure 2). In POME-based media, all nutrients including nitrogen, phosphorus, trace elements (except Si), and any essential vitamins were provided by POME. A medium with 10% POME was apparently deficient in some, or all, essential nutrients compared to the control medium and the media with 20% POME. Therefore, media with 10% POME did not support good biomass growth. Macronutrients such as N, P, and Si are known to be required for building essential cellular components (nucleic acids, phospholipids, chlorophyll, proteins, cell wall), therefore, a deficiency in any of them could reduce biomass growth and final concentration, consistent with the observations in media with less than 20% POME and less than 80 μM Na_2SiO_3 (Figure 2A,B). Photosynthesis, chlorophyll biosynthesis, and protein biosynthesis have been shown to be down-regulated in both N- and P-deficient cells of *T. pseudonana* [67], consistent with the observed poor biomass production in media with <10% POME (Figure 1).

If a medium with 20% POME provided sufficient nutrients, a higher concentration of POME should have provided more and was expected to better support biomass growth. In contrast, a high POME level (>20% by volume) adversely impacted growth and the final biomass concentration (Figure 2). This was consistent with other similar observations about media with too high a level of POME [10]. Because of its dark color, too high a concentration of POME reduces light penetration and, therefore, biomass production [10,68]. In addition, if used in a high concentration, certain components in POME inhibit the growth of microalgae and other microorganisms [14–16,68]. The colored inhibitors include dissolved tannins, lignins, and other similar organics [10].

The possible presence of vitamins in POME is explained by the many soil microorganisms that naturally grow in it [10]. Many such microbes are known to produce vitamins, particularly the B-group vitamins. Standard f/2 includes only three vitamins: vitamin B12, vitamin B7 (biotin), and vitamin B1 (thiamine). Although POME was sterilized prior to use, B vitamins such as B12 and B7 are known to be highly heat stable whereas B1 is reasonably heat stable. Therefore, sterilization was unlikely to have had much effect on the concentration of the three specified B vitamins that may have been originally present.

Both in the control medium and the media formulated with 20% POME, the final biomass concentration increased as the initial sodium silicate concentration was increased from 40 μM to 80 μM (Figure 2A,B). Therefore, both these media were limiting in silicate at an initial Na_2SiO_3 concentration of 40 μM. A supply of metabolizable silicon in the culture medium is essential for rapid growth and biomass accumulation, as it is required to build cell walls [69]. Silicon limitation affects not only cell wall synthesis, but also the cell cycle and frequency of cell division [70,71]. Under silicon stress, *T. pseudonana* may continue to grow for some time by reducing the silicon content of its frustule, although other diatoms may respond differently [72], in the absence of silicon *T. pseudonana* ceases to grow [71]. The diatom growth rate and final biomass concentration declined progressively in both the control medium and the 20% POME media as the initial Na_2SiO_3 in these media was increased to above 80 μM (Figure 2C,D). Therefore, too much silicon inhibited growth and an initial Na_2SiO_3 concentration of 80 μM was considered to be optimal for *T. pseudonana* grown under the conditions used.

Compared with the above-identified 80 μM optimal concentration of Na_2SiO_3, the natural diatom habitat of oceanic surface waters is low in Si (<20 μM silicate in most surface waters), thus limiting growth [24]. Silicate dissolved in water at neutral pH is mainly in the form of silicic acid ($Si(OH)_4$) and diatoms appear to take up silicon primarily in this form [73]. The observed optimal silicate concentration of 80 μM in the present work was comparable to concentrations found in nature in certain habitats. For example, in parts of the Southern Ocean, the surface concentration of silicic acid can be as high as 50–70 μM [74]. At different concentrations of silicic acid, growth may also be affected by concentration-

dependent differences in the mechanisms of silicon uptake. Under low concentrations of silicic acid (<30 μM), it is taken up by the cells mainly via silicic acid transport proteins, but diffusion becomes a contributing factor at higher concentrations [75]. A high rate of diffusive transport of silicic acid in media containing high levels of Si may interfere with the uptake of other essential nutrients, and this is a possible explanation for the observed inhibitory effect of excessive Si. The inhibitory effect of a high Si concentration has been previously observed also for some other diatoms [76].

In view of the above results, the optimal medium was taken to comprise 20% by volume POME, 80 μM Na_2SiO_3, and 35 g NaCl L^{-1} in water at pH ~7.7. This medium was used in all subsequent work.

3.3. Effect of Light–Dark Cycle on Biomass Production and Lipid Content

The effects of the light–dark cycle were evaluated using the above-identified optimal medium in 15-day batch cultures conducted at otherwise identical conditions (Section 2.4). The final biomass concentration depended on the photoperiod as shown in Table 3. The lipid content of the biomass also responded to changes in photoperiod (Table 3). A 16 h daily photoperiod provided a significantly higher final biomass concentration compared to a 24 h photoperiod (Table 3). Photoperiods shorter than 16 h daily adversely impacted biomass production (Table 3). The lipid content of the biomass grown under a 16 h daily photoperiod was the highest (46.2 ± 1.1%; Table 3). This was nearly 21% higher than the biomass grown under continuous light (Table 3). Thus, the optimal light–dark cycle with the optimal POME medium was 16:8 h:h (Table 3), as it maximized both the biomass productivity and the lipid content in the biomass.

Table 3. Dependence of biomass and lipid production on the light–dark cycle.

Parameter	Light–Dark Cycle (h:h)			
	24:0	**16:8**	**12:12**	**8:16**
Biomass concentration (mg L^{-1})	812 ± 11 ^{a}	869 ± 14 ^{b}	791 ± 15 ^{c}	451 ± 12 ^{d}
Biomass productivity (mg L^{-1} d^{-1})	54.1 ± 0.7 ^{a}	57.9 ± 0.9 ^{b}	52.7 ± 1.0 ^{a}	30.1 ± 2.7 ^{c}
Lipids in biomass (%, *w*/*w*)	38.1 ± 0.8 ^{a}	46.2 ± 1.1 ^{b}	35.7 ± 0.9 ^{c}	12.6 ± 1.1 ^{d}

Data are mean values ± standard deviation (n = 3) on day 15. Numbers with different superscript letters in the same row are statistically significantly different (95% confidence level) by *t*-test for two means.

A light–dark cycle is unavoidable in natural habitats of diatoms. In nature, photoperiod varies with geographic location and season. The habitat of *T. pseudonana* spans coastal waters worldwide as well as inland waters, including fresh and brackish [35–41]. An ability to colonize geographically widespread regions suggests a high adaptability of *T. pseudonana* to a broad range of photoperiods.

Diatoms differ in their responses to the light–dark cycle. Some freshwater diatoms, for example, have been shown to have a preference for a longer day length (light period ≥ 16 h) for growth whereas others grow better with a 12 h day length [77]. This was consistent with the present observations (Table 3) for *T. pseudonana*, a diatom found widely in freshwaters [35].

In other studies, *T. pseudonana* has shown the fastest growth rates under long photoperiods (24 h and 16 h light daily) at low to moderate light intensities (75–150 μmol photons m^{-2} s^{-1}) [78], but the cells were more susceptible to photoinhibition than cells grown at the same light level but with a shorter (8 h per day) light period. Thus, at a light level of ~300 μmol photons m^{-2} s^{-1}, a photoperiod of 16 h daily resulted in slower growth compared to a photoperiod of 8 h per day [78]. *T. pseudonana* has been claimed to not require a daily dark period to achieve maximum specific growth rate [78], but some other *Thalassiosira* species do require a dark period daily for maximum growth performance [78]. All these studies concerning the lack of a need for a dark period were performed in purely photoautotrophic cultures, unlike the present case.

Response to the light–dark cycle differs among different species of *Thalassiosira*. For example, *Thalassiosira weissflogii* cells divided during both the light and dark phases of the light–dark cycle, and the growth rates did not differ significantly in these phases [38,79]. In contrast, in *Thalassiosira fluviatilis*, the specific growth rate progressively increased during the light phase and progressively declined during the dark part of the light–dark cycle (10 h light, 14 h dark) [80]. These observations related to purely photoautotrophic growth. In media containing metabolizable organic carbon, as in the present work, growth can be maintained heterotrophically in the dark; thus the total actual growth period is longer during a 15-day light–dark cycled batch culture, compared to an equivalent photoautotrophic culture.

In 13 species of marine phytoplankton grown under a 14:10 h/h light–dark cycle, cyclic oscillations in growth rates were detected in some species, but not others [81]. In some species cell division was clearly favored during light. In *T. pseudonana*, the specific growth rate tended to increase during light and decline during dark [81]. This decline in growth in the dark may not occur under heterotrophic conditions where both an assimilable carbon source is available in POME-containing media and oxygen is being continuously provided through aeration, as was the case in the present work.

For 22 marine microalgae species tested over a broad range of irradiance values, some failed to grow under continuous light although they grew well at all irradiance levels under a 14:10 h/h light–dark cycle [82]. Some reproduced slower in continuous light compared to growth under a 14:10 h/h light–dark cycle [82]. For all light levels, *T. pseudonana* grew more rapidly under continuous light than under a 14:10 h/h light–dark cycle [82] in purely photoautotrophic culture.

The need for a dark period in purely photoautotrophic cultures of certain species is often explained by the need to regenerate the photosystem II (PSII). PSII is essential for photosynthesis. It is also the most light-sensitive component of the photosynthetic machinery. PSII is continuously deactivated by light and is continuously produced. The concentration of PSII in *T. pseudonana* cells is inversely related to the prevailing light level [83]. PSII inactivation ceases in the dark and a pool of this protein may be accumulated during the dark to enhance the photosynthetic competency of the cells during the next light period. Light-induced deactivation of PSII ceases to be adequately compensated by synthesis of new PSII once the light level exceeds the saturating value (~400 μmol photons m^{-2} s^{-1} in *T. pseudonana* [44]). In the present study, the incident light level was around 50% of the saturation value, therefore severe damage to PSII was unlikely.

Under laboratory conditions, although the incident light level on the surface of a culture may be constant, the cells in a continuously mixed dense suspension experience fluctuating light as they move from a better illuminated region at the walls of a culture vessel to deeper in the fluid [84]. Diatoms are apparently better at acclimatizing to such rapid light–dark cycling compared to other phytoplankton such as dinoflagellates [85]. This ability to rapidly acclimatize is linked to the ability of the diatoms to produce certain proteins (e.g., Proton Gradient Regulation 5, PGR5 [85]) that some other algae cannot produce. The innate ability to adapt to rapidly fluctuating light may also translate into better adaptability to changes in the daily light cycle. The ability of *T. pseudonana* to colonize geographically wide-ranging habitats suggests an excellent adaptability to different light–dark cycles, but this does not imply the same biomass productivity under the different diurnal cycles.

In some diatoms, light has been suggested as a regulator of the cell cycle [86]. In many species, growth and cell division are closely tied to the diurnal light cycle although different species show different responses [82,87]. Depending on the species, the cell division occurs towards the end of the daily light period but may occur during the dark period [87]. The situation may be quite different in the presence of a metabolizable carbon source allowing growth in the dark, as was the case in the present work.

3.4. Biomass and Lipid Production under Optimal Conditions

Under the optimal light–dark cycle of 16:8 h/h, the biomass productivity in the present study was 57.9 ± 0.9 mg L^{-1} d^{-1} (Table 3). This was significantly higher (95% confidence level) than the productivity under continuous light. All biomass productivity data in Table 3 were high compared to many other reports for diatoms. For example, for 17 different marine diatoms grown in batch culture under identical conditions (standard f/2 medium, 20 °C, 200 µmol m^{-2} s^{-1} irradiance, 14:10 h/h light–dark cycle), the biomass productivity was found to range from 2.5 to 27.3 mg L^{-1} d^{-1} [17] under photoautotrophic growth. Under these conditions, the productivity of *T. pseudonana* was 5.9 mg L^{-1} d^{-1} [17]. In contrast with this, the lowest productivity in Table 3 was nearly 5-fold greater. This difference was explained by a combination of a higher culture temperature (26 °C) of the present work compared to 20 °C used in photoautotrophic cultures by d'Ippolito et al. [17] and the heterotrophic nutrition made possible by the use of POME. The growth rate has been reported to increase with temperature [42]. A 1.9-fold higher biomass productivity than observed by d'Ippolito et al. [17] at 20 °C (see above), was reported by Joseph et al. [88] for a *Thalassiosira* sp. grown photoautotrophically at ~25 °C. The other growth conditions (f/2 medium, continuous light at ~180 µmol m^{-2} s^{-1}) were similar to those used by d'Ippolito et al. [17]. Although the culture temperature used in the present work was almost the same as that used by Joseph et al. [88], the minimum biomass productivity in the present study (Table 3) was 2.6-fold higher most likely because of the contribution of heterotrophic nutrition.

For the biomass grown in the optimal POME medium under the optimal light–dark cycle, the lipid content in the biomass was 46.2 ± 1.1% (Table 3). This value was nearly 21% higher than the lipid level obtained under continuous light (Table 3). The observed lipid content (Table 3) was generally higher than most published reports for marine diatoms. For example, for several other marine diatoms, the lipid content in the photoautotrophically grown biomass was reported to range from 2.4% to 21.3% [89], but a lipid level of ~30% in the biomass was reported for a *Thalassiosira* sp. [88]. Similarly, measurements in 12 marine diatoms grown photoautotrophically under different conditions showed the total lipid content in the biomass to range from 30.2% to 45.1% [90]. Although higher lipid contents have been reported in a few diatoms [10,11], no prior reports with a lipid content as high as 46.2% (Table 3) were found for *T. pseudonana* possibly because prior studies all focused on the photoautotrophic mode of growth. An earlier study of two clones of *T. pseudonana* grown in f/2 medium reported a total lipid content of <22% by weight in dry biomass [91]. The cells were grown at 18 °C (14:10 h/h light–dark cycle, ~78 µmol photons m^{-2} s^{-1} light level) for 18 days [91]. The final biomass concentration was 78.6 mg L^{-1} corresponding to a productivity of ~4.4 mg L^{-1} d^{-1}.

The lipid content in *T. pseudonana* is known to increase under growth-suppressing nutrient stresses [92,93]. Nitrogen starvation enhances the accumulation of storage lipids, particularly triacylglycerols [92] and phosphorous stress also elevates the levels of certain lipids [93]. In 20% POME optimal medium, the culture was always well into the stationary phase by day 12 (Figure 2B), suggesting possible exhaustion of some nutrient (e.g., N, P) supplied by POME. Carbon was never limiting, as the cultures were continuously supplied with carbon dioxide. Therefore, the exceptionally high lipid content in the biomass (46.2%; Table 3) may have been a consequence of the cells being in a lipid-accumulating phase under nutritional stress.

3.5. Fatty Acid Methyl Esters in Biodiesel

The fatty acid methyl ester content in biodiesel is shown in Figure 3. The five main saturated fatty acids (myristic acid (14:0), pentadecanoic acid (15:0), palmitic acid (16:0), heptadecanoic acid (17:0), and stearic acid (18:0)) comprised 40.0% of the biodiesel. The five main monounsaturated fatty esters (methyl esters of myristoleic acid (14:1), palmitoleic acid (16:1), oleic acid (18:1), eicosenoic acid (20:1), and erucic acid (22:1)) comprised 48.9% of the total. The remaining 11.1% of the methyl esters were derived from the three main

polyunsaturated fatty acids (linoleic acid (18:2), linolenic acid (18:3), and docosahexaenoic acid (22:6)). The three most abundant fatty acids in the biodiesel were palmitoleic acid (31.6%), myristic acid (16.8%), and heptadecanoic acid (13.3%). The other main fatty acids included myristoleic acid (7.9%) and linoleic acid (5.8%). All other fatty acids were present at well below 5%.

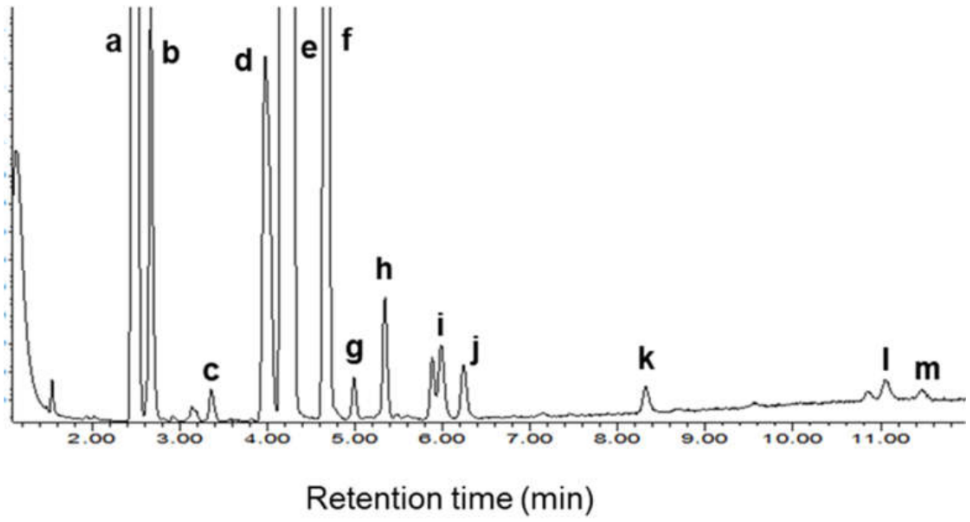

Figure 3. Chromatogram of transesterified fatty acids: myristic acid, 14:0 (a); myristoleic acid, 14:1 (b); pen-tadecanoic acid, 15:0 (c); palmitic acid, 16:0 (d); palmitoleic acid, 16:1 (e); heptadecanoic acid, 17:0 (f); stearic acid, 18:0 (g); oleic acid, 18:1 (h); linoleic acid, 18:2 (i); linolenic acid, 18:3 (j); eicosenoic acid, 20:1 (k); erucic acid, 22:1 (l); docosahexaenoic acid, 22:6 (m).

In conventional non-POME media, in addition to the fatty acids identified in the present work, *T. pseudonana* has been shown to produce long-chain polyunsaturated fatty acids such as eicosapentaenoic acid (EPA) and docosahexaenoic acid (DHA) under suitable conditions [33,48,49,94–96]. A significant proportion (e.g., 15–20%) of total lipids may be EPA and DHA, depending on the culture conditions. A relatively low culture temperature (e.g., 18–20 °C) elevates the levels of highly unsaturated fatty acids in *T. pseudonana* [95] as well as in many marine microorganisms [10,97,98], as previously explained [10,11,98]. For the purpose of making biodiesel, however, a high concentration of polyunsaturated fatty acids in the lipids is not wanted as they reduce the oxidative stability of biodiesel.

Although this was not examined, the composition of fatty acids in total diatomic lipids is also affected by the light level, the photoperiod, and whether growth is photoautotrophic or heterotrophic [97,99,100]. The fatty acid composition data in the present work were measured in the stationary phase, but the composition does depend somewhat on the phase of growth. For *T. pseudonana* grown in a seawater medium at 18 °C (constant illumination at 240 μmol m^{-2} s^{-1}), the ratio of unsaturated to saturated fatty acids was 1.65 in the exponential growth phase but 1.17 in the stationary growth phase [33]. In the present work, the ratio of unsaturated to saturated fatty acids (data in Table 4) was 1.5. This was comparable to data previously reported for the exponential phase of photoautotrophic growth of this diatom [33], but other studies [48,49] have shown high levels of polyunsaturated fatty acids in lipids of *T. pseudonana* (Table 4). For example, ratios of unsaturated to saturated fatty acids as high as 3.39 [48] and 2.65 [49] (Table 4) have been observed.

A low proportion of polyunsaturated fatty acids in total lipids in the present study was apparently a consequence of a relatively high culture temperature (26 °C) compared to most other studies [33,48,49] where the culture temperature had been 18–20 °C. An increase in culture temperature from 20 °C to 30 °C has previously been found to change the proportions of the different classes of fatty acids in the lipids of photoautorophically grown *T. pseudonana* (f/2 medium, 14-day batch culture, 80–100 μmol photons m^{-2} s^{-1}, 12:12 h:h light–dark cycle) [48]. The proportion of the saturated fatty acids increased, and both

monounsaturated and polyunsaturated fatty acids decreased as the culture temperature was raised [48]. The total lipid level of the biomass grown at 20 °C was only 16% [48], or only ~45% of the level observed in the present work with a 12:12 h:h light–dark cycle (Table 3).

Table 4. Percentages of different fatty acid classes [a] in total fatty acids of *T. pseudonana*.

Fatty Acid Class	This Work [b]	Mai et al. [48] [c]	Volkman et al. [49] [d]
Saturated	40.0	22.8	27.4
Monounsaturated	48.9	30.0	19.6
Polyunsaturated	11.1	47.2	53.0

[a] All data were based on the total fatty acids being the sum of saturated, monounsaturated, and polyunsaturated fatty acids. Non-fatty acid components were not included. [b] Grown mixotrophically in 20% POME medium (80 μM Na_2SiO_3 and 35 g NaCl L^{-1}; 26 ± 1 °C, 15 days; 16:8 h:h light–dark cycle, 200 μmol photons m^{-2} s^{-1}). [c] Grown photoautotrophically in f/2 medium (20 °C, 14 days, 80–100 μmol photons m^{-2} s^{-1}, 12:12 h:h light–dark cycle). [d] Grown photoautotrophically in f/2 medium (20 °C, 70–80 μmol photons m^{-2} s^{-1}, 12:12 h:h light–dark cycle; the cells were harvested in the late exponential growth phase).

4. Conclusions

For the marine diatom *Thalassiosira pseudonana* isolated from the Kuantan coastal region of peninsular Malaysia, growth in a POME-based medium was as good as in a standard control medium. The optimal POME-based medium contained 20% by volume POME, 80 μM Na_2SiO_3, and 35 g NaCl L^{-1} in distilled water at pH ~7.7. The highest biomass productivity in this medium in a 15-day batch culture (a 16:8 h:h light–dark cycle; illumination at 200 μmol photons m^{-2} s^{-1}, 26 ± 1 °C; continuous bubbling with CO_2-enriched air) was ~58 mg L^{-1} day^{-1}. The biomass had a lipid content of ~46% by dry weight and the lipid comprised mainly (~40%) monounsaturated fatty acids. Compared to the optimal 16 h:8 h light–dark cycle, continuous illumination under otherwise identical conditions reduced the biomass productivity by 6.6%, and the lipid content of the biomass was reduced by 17.5%. A POME concentration of >20% by volume in the culture medium inhibited biomass growth.

Author Contributions: K.M.P.: investigation; methodology; writing—original draft. G.P.M.: funding acquisition. A.Z.S.: methodology. M.H.A.R.: project administration. N.G.: investigation; methodology; verification; writing—original draft. Y.C.: supervision; visualization; writing—review and editing. All authors have read and agreed to the published version of the manuscript.

Funding: This study was funded by the Universiti Malaysia Pahang (UMP) through the UMP Flagship Grant (RDU182205) and Internal Research Grants (RDU1903125 and RDU190337).

Institutional Review Board Statement: Not applicable.

Informed Consent Statement: Not applicable.

Data Availability Statement: All relevant data are within the paper.

Acknowledgments: The authors gratefully acknowledge Universiti Malaysia Pahang (UMP) for financial support through the UMP Flagship Grant (RDU182205) and Internal Research Grants (RDU1903125 and RDU190337).

Conflicts of Interest: The authors declare no conflict of interest.

References

1. Kamyab, H.; Chelliapan, S.; Din, M.F.M.; Rezania, S.; Khademi, T.; Kumar, A. *Palm Oil Mill Effluent as an Environmental Pollutant*; IntechOpen: London, UK, 2018. [CrossRef]
2. Poh, P.E.; Yong, W.-J.; Chong, M.F. Palm oil mill effluent (POME) characteristic in high crop season and the applicability of high-rate anaerobic bioreactors for the treatment of POME. *Ind. Eng. Chem. Res.* **2010**, *49*, 11732–11740. [CrossRef]
3. Bux, F.; Chisti, Y. (Eds.) *Algae Biotechnology: Products and Processes*; Springer: New York, NY, USA, 2016. [CrossRef]
4. Chisti, Y. Society and microalgae: Understanding the past and present. In *Microalgae in Health and Disease Prevention*; Levine, I.A., Fleurence, J., Eds.; Academic Press: London, UK, 2018; pp. 11–21. [CrossRef]

5. Chisti, Y. Microalgae biotechnology: A brief introduction. In *Handbook of Microalgae-Based Processes and Products: Fundamentals and Advances in Energy, Food, Feed, Fertilizer, and Bioactive Compounds*; Jacob-Lopes, E., Maroneze, M.M., Queiroz, M.I., Zepka, L.Q., Eds.; Academic Press: London, UK, 2020; pp. 3–23. [CrossRef]
6. Pandey, A.; Lee, D.J.; Chang, J.S.; Chisti, Y.; Soccol, C.R. (Eds.) *Biomass, Biofuels, Biochemicals: Biofuels from Algae*; Elsevier: New York, NY, USA, 2018. [CrossRef]
7. Wang, J.K.; Seibert, M. Prospects for commercial production of diatoms. *Biotechnol. Biofuels* **2017**, *10*, 16. [CrossRef]
8. Lim, C.I.; Biswas, W. Sustainability assessment for crude palm oil production in Malaysia using the palm oil sustainability assessment framework. *Sust. Dev.* **2019**, *27*, 253–269. [CrossRef]
9. Palanisamy, K.M.; Paramasivam, P.; Jayakumar, S.; Maniam, G.P.; Rahim, M.H.A.; Govindan, N. Economical cultivation system of microalgae *Spirulina platensis* for lipid production. *IOP Conf. Ser. Earth Environ. Sci.* **2021**, *641*, 012022. [CrossRef]
10. Palanisamy, K.M.; Paramasivam, P.; Maniam, G.P.; Rahim, M.H.A.; Govindan, N.; Chisti, Y. Production of lipids by *Chaetoceros affinis* in media based on palm oil mill effluent. *J. Biotechnol.* **2021**, *327*, 86–96. [CrossRef]
11. Govindan, N.; Maniam, G.P.; Yusoff, M.M.; Rahim, M.H.A.; Chatsungnoen, T.; Ramaraj, R.; Chisti, Y. Statistical optimization of lipid production by the diatom *Gyrosigma* sp. grown in industrial wastewater. *J. Appl. Phycol.* **2020**, *32*, 375–387. [CrossRef]
12. Govindan, N.; Maniam, G.P.; Sulaiman, A.Z.; Ajit, A.; Chatsungnoen, T.; Chisti, Y. Production of renewable lipids by the diatom *Amphora copulata*. *Fermentation* **2021**, *7*, 37. [CrossRef]
13. Jayakumar, S.; Bhuyar, P.; Pugazhendhi, A.; Rahim, M.H.A.; Maniam, G.P.; Govindan, N. Effects of light intensity and nutrients on the lipid content of marine microalga (diatom) *Amphiprora* sp. for promising biodiesel production. *Sci. Total Environ.* **2021**, *768*, 145471. [CrossRef]
14. Jasni, J.; Arisht, S.N.; Yasin, N.H.M.; Abdul, P.M.; Lin, S.-K.; Liu, C.-M.; Wu, S.-Y.; Jahim, J.M.; Takriff, M.S. Comparative toxicity effect of organic and inorganic substances in palm oil mill effluent (POME) using native microalgae species. *J. Water Process Eng.* **2020**, *34*, 101165. [CrossRef]
15. Kamyab, H.; Din, M.F.M.; Keyvanfar, A.; Majid, M.Z.A.; Talaiekhozani, A.; Shafaghat, A.; Lee, C.T.; Shiun, L.J.; Ismail, H.H. Efficiency of microalgae *Chlamydomonas* on the removal of pollutants from palm oil mill effluent (POME). *Energy Procedia* **2015**, *75*, 2400–2408. [CrossRef]
16. Nur, M.M.A.; Setyoningrum, T.M.; Budiaman, G.S. Potency of *Botryococcus braunii* cultivated on palm oil mill effluent wastewater as a source of biofuel. *Environ. Eng. Res.* **2017**, *22*, 417–425. [CrossRef]
17. d'Ippolito, G.; Sardo, A.; Paris, D.; Vella, F.M.; Adelfi, M.G.; Botte, P.; Gallo, C.; Fontana, A. Potential of lipid metabolism in marine diatoms for biofuel production. *Biotechnol. Biofuels* **2015**, *8*, 28. [CrossRef]
18. Savio, S.; Farrotti, S.; Paris, D.; Arnaìz, E.; Díaz, I.; Bolado, S.; Muñoz, R.; Rodolfo, C.; Congestri, R. Value-added co-products from biomass of the diatoms *Staurosirella pinnata* and *Phaeodactylum tricornutum*. *Algal Res.* **2020**, *47*, 101830. [CrossRef]
19. Maeda, Y.; Nojima, D.; Yoshino, T.; Tanaka, T. Structure and properties of oil bodies in diatoms. *Philos. Trans. R. Soc. B* **2017**, *372*, 20160408. [CrossRef]
20. Paasche, E. Silicon and the ecology of marine plankton diatoms. I. Thalassiosira pseudonana (Cyclotella nana) grown in a chemostat with silicate as limiting nutrient. *Mar. Biol.* **1973**, *19*, 117–126. [CrossRef]
21. Armbrust, E.V.; Berges, J.A.; Bowler, C.; Green, B.R.; Martinez, D.; Putnam, N.H.; Zhou, S.; Allen, A.E.; Apt, K.E.; Bechner, M.; et al. The genome of the diatom *Thalassiosira pseudonana*: Ecology, evolution, and metabolism. *Science* **2004**, *306*, 79–86. [CrossRef]
22. Ahmad, A.; Tiwari, A.; Srivastava, S. A genome-scale metabolic model of *Thalassiosira pseudonana* CCMP 1335 for a systems-level understanding of its metabolism and biotechnological potential. *Microorganisms* **2020**, *8*, 1396. [CrossRef]
23. Hildebrand, M. Diatoms, biomineralization processes, and genomics. *Chem. Rev.* **2008**, *108*, 4855–4874. [CrossRef]
24. Martin-Jézéquel, V.; Hildebrand, M.; Brzezinski, M.A. Silicon metabolism in diatoms: Implications for growth. *J. Phycol.* **2000**, *36*, 821–840. [CrossRef]
25. Villanova, V.; Spetea, C. Mixotrophy in diatoms: Molecular mechanism and industrial potential. *Physiol. Plant.* **2021**, *173*, 603–611. [CrossRef]
26. Baldisserotto, C.; Sabia, A.; Guerrini, A.; Demaria, S.; Maglie, M.; Ferroni, L.; Pancaldi, S. Mixotrophic cultivation of *Thalassiosira pseudonana* with pure and crude glycerol: Impact on lipid profile. *Algal Res.* **2021**, *54*, 102194. [CrossRef]
27. Menegol, T.; Romero-Villegas, G.I.; López-Rodríguez, M.; Navarro-López, E.; López-Rosales, L.; Chisti, Y.; Molina-Grima, E. Mixotrophic production of polyunsaturated fatty acids and carotenoids by the microalga *Nannochloropsis gaditana*. *J. Appl. Phycol.* **2019**, *31*, 2823–2832. [CrossRef]
28. Ashworth, J.; Coesel, S.; Lee, A.; Armbrust, E.V.; Orellana, M.V.; Baliga, N.S. Genome-wide diel growth state transitions in the diatom *Thalassiosira pseudonana*. *Proc. Natl. Acad. Sci. USA* **2013**, *110*, 7518–7523. [CrossRef]
29. Ferguson, R.L.; Collier, A.; Meeter, D.A. Growth response of *Thalassiosira pseudonana* Hasle and Heimdal clone 3H to illumination, temperature and nitrogen source. *Chesapeake Sci.* **1976**, *17*, 148–158. [CrossRef]
30. León-Saiki, G.M.; Remmers, I.M.; Martens, D.E.; Lamers, P.P.; Wijffels, R.H.; van der Veen, D. The role of starch as transient energy buffer in synchronized microalgal growth in *Acutodesmus obliquus*. *Algal Res.* **2017**, *25*, 160–167. [CrossRef]
31. Dong, H.-P.; Dong, Y.-L.; Cui, L.; Balamurugan, S.; Gao, J.; Lu, S.-H.; Jiang, T. High light stress triggers distinct proteomic responses in the marine diatom *Thalassiosira pseudonana*. *BMC Genom.* **2016**, *17*, 994. [CrossRef]

32. Vásquez-Suárez, A.; Guevara, M.; González, M.; Cortez, R.; Arredondo-Vega, B. Crecimiento y composición bioquímica de *Thalassiosira pseudonana* (Thalassiosirales: Thalassiosiraceae) bajo cultivo semi-continuo en diferentes medios y niveles de irradiancies. (Growth and biochemical composition of *Thalassiosira pseudonana* (Thalassiosirales: Thalassiosiraceae) cultivated in semicontinuous system at different culture media and irradiances). *Rev. Biol. Trop.* **2013**, *61*, 1003–1013.
33. Tonon, T.; Harvey, D.; Larson, T.R.; Graham, I.A. Long chain polyunsaturated fatty acid production and partitioning to triacylglycerols in four microalgae. *Phytochemistry* **2002**, *61*, 15–24. [CrossRef]
34. Zhukova, N.V. Changes in the lipid composition of *Thalassiosira pseudonana* during its life cycle. *Russ. J. Plant Physiol.* **2004**, *51*, 702–707. [CrossRef]
35. Alverson, A.J.; Beszteri, B.; Julius, M.L.; Theriot, E.C. The model marine diatom *Thalassiosira pseudonana* likely descended from a freshwater ancestor in the genus *Cyclotella*. *BMC Evol. Biol.* **2011**, *11*, 125. [CrossRef]
36. Aké-Castillo, J.A.; Hernández-Becerril, D.U.; Meave del Castillo, M.E. Species of the genus *Thalassiosira* (Bacillariophyceae) from the Gulf of Tehuantepec, Mexico. *Bot. Mar.* **1999**, *42*, 487–503. [CrossRef]
37. Gastineau, R.; Hamedi, C.; Hamed, M.B.B.; Abi-Ayad, S.-M.-A.; Bąk, M.; Lemieux, C.; Turmel, M.; Dobosz, S.; Wróbel, R.J.; Kierzek, A.; et al. Morphological and molecular identification reveals that waters from an isolated oasis in Tamanrasset (extreme South of Algerian Sahara) are colonized by opportunistic and pollution-tolerant diatom species. *Ecol. Indic.* **2021**, *121*, 107104. [CrossRef]
38. Kipp, R.M.; Mccarthy, M.; Fusaro, A. Thalassiosira pseudonana (Hustedt) Hasle and Heimdal, (1957) 1970: U.S Geological Survey, Nonindigenous Aquatic Species Database, Gainesville, FL, and NOAA Great Lakes Aquatic Nonindigenous Species Information System, Ann Arbor, MI. Revision Date: 9/12/2019. Available online: https://nas.er.usgs.gov/queries/GreatLakes/FactSheet.aspx?SpeciesID=1692 (accessed on 2 November 2021).
39. Kiss, K.T. Occurrence of *Thalassiosira pseudonana* new record Bacillariophyceae in some rivers of Hungary. *Acta Bot. Hung.* **1984**, *30*, 277–288.
40. Lowe, R.L.; Busch, D.E. Morphological observations on two species of the diatom genus *Thalassiosira* from fresh-water habitats in Ohio. *Trans. Am. Microsc. Soc.* **1975**, *94*, 118–123. [CrossRef]
41. Muylaert, K.; Sabbe, K. The diatom genus *Thalassiosira* (Bacillariophyta) in the estuaries of the Schelde (Belgium/The Netherlands) and the Elbe (Germany). *Bot. Mar.* **1996**, *39*, 103–115. [CrossRef]
42. Gleich, S.J.; Plough, L.V.; Glibert, P.M. Photosynthetic efficiency and nutrient physiology of the diatom *Thalassiosira pseudonana* at three growth temperatures. *Mar. Biol.* **2020**, *167*, 124. [CrossRef]
43. Sabia, A.; Clavero, E.; Pancaldi, S.; Rovira, J.S. Effect of different CO_2 concentrations on biomass, pigment content, and lipid production of the marine diatom *Thalassiosira pseudonana*. *Appl. Microbiol. Biotechnol.* **2018**, *102*, 1945–1954. [CrossRef]
44. Hewes, C.D. Timing is everything: Optimizing crop yield for *Thalassiosira pseudonana* (Bacillariophyceae) with semi-continuous culture. *J. Appl. Phycol.* **2016**, *28*, 3213–3223. [CrossRef]
45. Price, N.M.; Thompson, P.A.; Harrison, P.J. Selenium: An essential element for growth of the coastal marine diatom *Thalassiosira pseudonana* (Bacillariophyceae). *J. Phycol.* **1987**, *23*, 1–9. [CrossRef]
46. Doucette, G.J.; Price, N.M.; Harrison, P.J. Effects of selenium deficiency on the morphology and ultrastructure of the coastal marine diatom *Thalassiosira pseudonana* (Bacillariophyceae). *J. Phycol.* **1987**, *23*, 9–17. [CrossRef]
47. Cong, N.V.; Vien, D.T.H.; Hong, D.D. Fatty acid profile and nutrition values of the microalga (*Thalassiosira pseudonana*) used in white shrimp culture. *Vietnam J. Sci. Technol.* **2018**, *56*, 138–145.
48. Mai, T.D.; Lee-Chang, K.J.; Jameson, I.D.; Hoang, T.; Cai, N.B.A.; Pham, H.Q. Fatty acid profiles of selected microalgae used as live feeds for shrimp postlarvae in Vietnam. *Aquacult. J.* **2021**, *1*, 26–38. [CrossRef]
49. Volkman, J.K.; Jeffrey, S.W.; Nichols, P.D.; Rogers, G.I.; Garlan, C.D. Fatty acid and lipid composition of 10 species of microalgae used in mariculture. *J. Exp. Mar. Biol. Ecol.* **1989**, *128*, 219–240. [CrossRef]
50. Blanco, S. Diatom taxonomy and identification keys. In *Modern Trends in Diatom Identification*; Cristobal, G., Blanco, S., Bueno, G., Eds.; Springer: Cham, Switzerland, 2020; pp. 25–38. [CrossRef]
51. Hustedt, F. *Die Süsswasser-Flora Mitteleuropas: Heft 10: Bacillariophyta (Diatomeae)*, 2nd ed.; Verlag Von Gustav Fischer: Jena, Germany, 1930; p. 466.
52. Hendey, N.I. *An Introductory Account of the Smaller Algae of British Coastal Waters, Part V, Bacillariophyceae (Diatoms)*; HMSO: London, UK, 1964.
53. Wehr, J.D.; Sheath, R.G. *Freshwater Algae of North America: Ecology and Classification*; Academic Press: London, UK, 2003. [CrossRef]
54. Taylor, J.C.; Harding, W.R.; Archibald, C.G.M. *A Methods Manual for the Collection, Preparation and Analysis of Diatom Samples*; WRC Report No TT 281/07; Water Research Commission: Pretoria, South Africa, 2007.
55. Hasle, G.R. Examination of diatom type material: *Nitzschia delicatissima* Cleve, *Thalassiosira minuscula* Krasske, and *Cyclotella nana* Hustedt. *Br. Phycol. J.* **1976**, *11*, 101–110. [CrossRef]
56. Rea, I.; Terracciano, M.; Chandrasekaran, S.; Voelcker, N.H.; Dardano, P.; Martucci, N.M.; De Stefano, L. Bioengineered silicon diatoms: Adding photonic features to a nanostructured semiconductive material for biomolecular sensing. *Nanoscale Res. Lett.* **2016**, *11*, 405. [CrossRef]
57. Guillard, R.R.L.; Lorenzen, C.J. Yellow-green algae with chlorophyllide C^{12}. *J. Phycol.* **1972**, *8*, 10–14. [CrossRef]
58. American Public Health Association. *Standard Methods for the Examination of Water and Wastewater*; American Public Health Association: Washington, DC, USA, 1999.

59. Neoh, C.H.; Lam, C.Y.; Ghani, S.M.; Ware, I.; Sarip, S.H.M.; Ibrahim, Z. Bioremediation of high-strength agricultural wastewater using *Ochrobactrum* sp. strain SZ1. *3 Biotech* **2016**, *6*, 143. [CrossRef]
60. Manaf, I.S.A.; Rahim, M.H.A.; Govindan, N.; Maniam, G.P. A first report on biodiesel production from *Aglaia korthalsii* seed oil using waste marine barnacle as a solid catalyst. *Ind. Crops Prod.* **2018**, *125*, 395–400. [CrossRef]
61. Malek, M.N.F.A.; Veerappan, V.; Rahim, M.H.A.; Maniam, G.P. Various adsorbents to improve the filterability of biodiesel. *Phys. Chem. Earth* **2020**, *120*, 102910. [CrossRef]
62. Manaf, I.S.A.; Yi, C.J.; Rahim, M.H.A.; Maniam, G.P. Utilization of waste fish bone as catalyst in transesterification of RBD palm oil. *Mater. Today Proc.* **2019**, *19*, 1294–1302. [CrossRef]
63. Hogan, P.; Otero, P.; Murray, P.; Saha, S.K. Effect of biomass pre-treatment on supercritical CO_2 extraction of lipids from marine diatom *Amphora* sp. and its biomass evaluation as bioethanol feedstock. *Heliyon* **2021**, *7*, e05995. [CrossRef]
64. Hildebrand, M.; York, E.; Kelz, J.I.; Davis, A.K.; Frigeri, L.G.; Allison, D.P.; Doktycz, M.J. Nanoscale control of silica morphology and three-dimensional structure during diatom cell wall formation. *J. Mater. Res.* **2006**, *21*, 2689–2698. [CrossRef]
65. Thamatrakoln, K.; Hildebrand, M. Analysis of *Thalassiosira pseudonana* silicon transporters indicates distinct regulatory levels and transport activity through the cell cycle. *Eukaryot. Cell* **2007**, *6*, 271–279. [CrossRef]
66. Moore, E.R.; Bullington, B.S.; Weisberg, A.J.; Jiang, Y.; Chang, J.; Halsey, K.H. Morphological and transcriptomic evidence for ammonium induction of sexual reproduction in *Thalassiosira pseudonana* and other centric diatoms. *PLoS ONE* **2017**, *12*, e0181098. [CrossRef]
67. Chen, X.H.; Li, Y.Y.; Zhang, H.; Liu, J.L.; Xie, Z.X.; Lin, L.; Wang, D.Z. Quantitative proteomics reveals common and specific responses of a marine diatom *Thalassiosira pseudonana* to different macronutrient deficiencies. *Front. Microbiol.* **2018**, *9*, 2761. [CrossRef]
68. Cheah, W.Y.; Show, P.L.; Juan, J.C.; Chang, J.S.; Ling, T.C. Microalgae cultivation in palm oil mill effluent (POME) for lipid production and pollutants removal. *Energy Convers. Manag.* **2018**, *174*, 430–438. [CrossRef]
69. Mock, T.; Samanta, M.P.; Iverson, V.; Berthiaume, C.; Robison, M.; Holtermann, K.; Durkin, C.; BonDurant, S.S.; Richmond, K.; Rodesch, M.; et al. Whole-genome expression profiling of the marine diatom *Thalassiosira pseudonana* identifies genes involved in silicon bioprocesses. *Proc. Natl. Acad. Sci. USA* **2008**, *105*, 1579–1584. [CrossRef]
70. Brzezinski, M.A.; Olson, R.J.; Chisholm, S.W. Silicon availability and cell-cycle progression in marine diatoms. *Mar. Ecol. Prog. Ser.* **1990**, *67*, 83–96. [CrossRef]
71. Hildebrand, M.; Frigeri, L.G.; Davis, A.K. Synchronized growth of *Thalassiosira pseudonana* (Bacillariophyceae) provides novel insights into cell-wall synthesis processes in relation to the cell cycle. *J. Phycol.* **2007**, *43*, 730–740. [CrossRef]
72. McNair, H.M.; Brzezinski, M.A.; Krause, J.W. Diatom populations in an upwelling environment decrease silica content to avoid growth limitation. *Environ. Microbiol.* **2018**, *20*, 4184–4193. [CrossRef]
73. Amo, Y.D.; Brzezinski, M.A. The chemical form of dissolved Si taken up by marine diatoms. *J. Phycol.* **1999**, *35*, 1162–1170. [CrossRef]
74. Cermeño, P.; Falkowski, P.G.; Romero, O.E.; Schaller, M.F.; Vallina, S.M. Continental erosion and the Cenozoic rise of marine diatoms. *Proc. Natl. Acad. Sci. USA* **2015**, *112*, 4239–4244. [CrossRef]
75. Shrestha, R.P.; Hildebrand, M. Evidence for a regulatory role of diatom silicon transporters in cellular silicon responses. *Eukaryot. Cell* **2015**, *14*, 29–40. [CrossRef]
76. Lewin, J.C. Silicon metabolism in diatoms. II. Sources of silicon for growth of *Navicula pelliculosa*. *Plant Physiol.* **1955**, *30*, 129–134. [CrossRef]
77. Sicko-Goad, L.; Andresen, N.A. Effect of growth and light/dark cycles on diatom lipid content and composition. *J. Phycol.* **1991**, *27*, 710–718. [CrossRef]
78. Li, G.; Talmy, D.; Campbell, D.A. Diatom growth responses to photoperiod and light are predictable from diel reductant generation. *J. Phycol.* **2017**, *53*, 95–107. [CrossRef]
79. Wu, Y.; Zeng, Y.; Qu, J.Y.; Wang, W.-X. Mercury effects on *Thalassiosira weissflogii*: Applications of two-photon excitation chlorophyll fluorescence lifetime imaging and flow cytometry. *Aquatic Toxicol.* **2012**, *110*, 133–140. [CrossRef]
80. Chisholm, S.W.; Costello, J.C. Influence of environmental factors and population composition on the timing of cell division in *Thalassiosira fluviatilis* (Bacillariophyceae) grown on light/dark cycles. *J. Phycol.* **1980**, *16*, 375–383. [CrossRef]
81. Nelson, D.M.; Brand, L.E. Cell division periodicity in 13 species of marine phytoplankton on a light: Dark cycle. *J. Phycol.* **1979**, *15*, 67–75. [CrossRef]
82. Brand, L.E.; Guillard, R.R.L. The effects of continuous light and light intensity on the reproduction rates of twenty-two species of marine phytoplankton. *J. Exp. Mar. Biol. Ecol.* **1981**, *50*, 119–132. [CrossRef]
83. Li, G.; Woroch, A.D.; Donaher, N.A.; Cockshutt, A.M.; Campbell, D.A. A hard day's night: Diatoms continue recycling photosystem II in the dark. *Front. Mar. Sci.* **2016**, *3*, 218. [CrossRef]
84. Camacho Rubio, F.; García Camacho, F.; Fernández Sevilla, J.M.; Chisti, Y.; Molina Grima, E. A mechanistic model of photosynthesis in microalgae. *Biotechnol. Bioeng.* **2003**, *81*, 459–473. [CrossRef]
85. Zhou, L.; Wu, S.; Gu, W.; Wang, L.; Wang, J.; Gao, S.; Wang, G. Photosynthesis acclimation under severely fluctuating light conditions allows faster growth of diatoms compared with dinoflagellates. *BMC Plant Biol.* **2021**, *21*, 164. [CrossRef]
86. Zachleder, V.; Bišová, K.; Vítová, M. The cell cycle of microalgae. In *The Physiology of Microalgae*; Borowitzka, M., Beardall, J., Raven, J., Eds.; Springer: Cham, Switzerland, 2016; pp. 3–46. [CrossRef]

87. Jacquet, S.; Partensky, F.; Lennon, J.F.; Vaulot, D. Diel patterns of growth and division in marine picoplankton in culture. *J. Phycol.* **2001**, *37*, 357–369. [CrossRef]
88. Joseph, M.M.; Renjith, K.R.; John, G.; Nair, S.M.; Chandramohanakumar, N. Biodiesel prospective of five diatom strains using growth parameters and fatty acid profiles. *Biofuels* **2017**, *8*, 81–89. [CrossRef]
89. Ying, L.; Mai, K.-S.; Sun, S.-C. Total lipid and fatty acid composition of eight strains of marine diatoms. *Chin. J. Oceanol. Limnol.* **2000**, *18*, 345–349. [CrossRef]
90. Chen, Y.-C. The biomass and total lipid content and composition of twelve species of marine diatoms cultured under various environments. *Food Chem.* **2012**, *131*, 211–219. [CrossRef]
91. Fisher, N.S.; Schwarzenbach, R.P. Fatty acid dynamics in *Thalassiosira pseudonana* (Bacillariophyceae): Implications for physiological ecology. *J. Phycol.* **1978**, *14*, 143–150. [CrossRef]
92. Bromke, M.A.; Giavalisco, P.; Willmitzer, L.; Hesse, H. Metabolic analysis of adaptation to short-term changes in culture conditions of the marine diatom *Thalassiosira pseudonana*. *PLoS ONE* **2013**, *8*, e67340. [CrossRef]
93. Hunter, J.E.; Brandsma, J.; Dymond, M.K.; Koster, G.; Moore, C.M.; Postle, A.D.; Mills, R.A.; Attard, G.S. Lipidomics of *Thalassiosira pseudonana* under phosphorus stress reveal underlying phospholipid substitution dynamics and novel diglycosylceramide substitutes. *Appl. Environ. Microbiol.* **2018**, *84*, e02034-17. [CrossRef]
94. Boelen, P.; van Mastrigt, A.; van de Bovenkamp, H.H.; Heeres, H.J.; Buma, A.G.J. Growth phase significantly decreases the DHA-to-EPA ratio in marine microalgae. *Aquacult. Int.* **2017**, *25*, 577–587. [CrossRef]
95. Cook, O.; Hildebrand, M. Enhancing LC-PUFA production in *Thalassiosira pseudonana* by overexpressing the endogenous fatty acid elongase genes. *J. Appl. Phycol.* **2016**, *28*, 897–905. [CrossRef]
96. Tonon, T.; Qing, R.; Harvey, D.; Li, Y.; Larson, T.R.; Graham, I.A. Identification of a long-chain polyunsaturated fatty acid acyl-coenzyme A synthetase from the diatom *Thalassiosira pseudonana*. *Plant Physiol.* **2005**, *138*, 402–408. [CrossRef]
97. Mortensen, S.H.; Børsheim, K.Y.; Rainuzzo, J.R.; Knutsen, G. Fatty acid and elemental composition of the marine diatom *Chaetoceros gracilis* Schütt. Effects of silicate deprivation, temperature and light intensity. *J. Exp. Mar. Biol. Ecol.* **1988**, *122*, 173–185. [CrossRef]
98. Shene, C.; Paredes, P.; Flores, L.; Leyton, A.; Asenjo, J.A.; Chisti, Y. Dynamic flux balance analysis of biomass and lipid production by Antarctic thraustochytrid *Oblongichytrium* sp. RT2316-13. *Biotechnol. Bioeng.* **2020**, *117*, 3006–3017. [CrossRef]
99. Opute, F.I. Lipid and fatty-acid composition of diatoms. *J. Exp. Bot.* **1974**, *25*, 823–835. [CrossRef]
100. Sicko-Goad, L.; Simmons, M.S.; Lazinsky, D.; Hall, J. Effect of light cycle on diatom fatty acid composition and quantitative morphology. *J. Phycol.* **1988**, *24*, 1–7. [CrossRef]